



UNIVERSITY OF LEEDS

This is a repository copy of *New concept to aid efficient fibre integration into metal matrices during ultrasonic consolidation*.

White Rose Research Online URL for this paper:
<http://eprints.whiterose.ac.uk/130049/>

Version: Accepted Version

Article:

Masurtschak, S, Friel, RJ and Harris, RA orcid.org/0000-0002-3425-7969 (2017) New concept to aid efficient fibre integration into metal matrices during ultrasonic consolidation. *Proceedings of the Institution of Mechanical Engineers, Part B: Journal of Engineering Manufacture*, 231 (7). pp. 1105-1115. ISSN 0954-4054

<https://doi.org/10.1177/0954405415592120>

© 2015, Author(s). This is an author produced version of a paper published in *Proceedings of the Institution of Mechanical Engineers, Part B: Journal of Engineering Manufacture*. Uploaded in accordance with the publisher's self-archiving policy.

Reuse

Items deposited in White Rose Research Online are protected by copyright, with all rights reserved unless indicated otherwise. They may be downloaded and/or printed for private study, or other acts as permitted by national copyright laws. The publisher or other rights holders may allow further reproduction and re-use of the full text version. This is indicated by the licence information on the White Rose Research Online record for the item.

Takedown

If you consider content in White Rose Research Online to be in breach of UK law, please notify us by emailing eprints@whiterose.ac.uk including the URL of the record and the reason for the withdrawal request.



eprints@whiterose.ac.uk
<https://eprints.whiterose.ac.uk/>

**New concept to aid efficient fibre integration into metal matrices during
Ultrasonic Consolidation**

Simona Masurtschak*, Ross J Friel, Russell A Harris

Wolfson School of Mechanical and Manufacturing Engineering, Loughborough
University, Loughborough, Leicestershire, LE11 3TU, UK

*Simona Masurtschak, Wolfson Building, Loughborough University, Ashby Road,
Loughborough, LE11 3TU, UK.

Email: s.masurtschak@lboro.ac.uk

Abstract

Ultrasonic consolidation has been shown to be a viable metal matrix based smart composite additive layer manufacturing process. Yet, high quantity fibre integration has presented the requirement for a method of accurate positioning and fibre protection to maintain the fibre layout during ultrasonic consolidation. This study presents a novel approach for fibre integration during ultrasonic consolidation: Channels are manufactured by laser processing on an ultrasonically consolidated sample. At the same time, controlled melt ejection is applied to aid accurate fibre placement and simultaneously reducing fibre damage occurrences. Microscopic, SEM and EDX analysis are used for samples containing up to 10.5% fibres, the

highest volume in an ultrasonically consolidated composite so far. Up to 98% of the fibres remain in the channels after consolidation and fibre damage is reduced to less than 2% per sample. This study furthers the knowledge of high volume fibre embedment via ultrasonic consolidation for future smart material manufacturing.

Keywords

Metal Matrix Composites (MMC), Ultrasonic Consolidation, Laser processing, Aluminium

Date received:

1. Introduction

Ultrasonic consolidation (UC) is an additive manufacturing method based on the ultrasonic welding of a sequence of metal foils. The process is suited to producing complex 3D metal parts by combining ultrasonic metal welding and Computer Numerical Control (CNC) milling techniques¹. A schematic overview of the process is given in Figure 1(a) and (b). The theory for bond formation that has the most consensus is currently atomic bonding^{2,3} and is displayed in Figure 1(c) to (e). The foil surfaces, comprising of oxide layers and asperities, are brought into contact by the contact pressure of the sonotrode and anvil. The oscillating shear forces generate friction at the interface which causes the impure surface structures to be

broken-up and dispersed along the weld line. Plastic deformation causes new material to be extruded from underneath which forms the metallurgical bond.

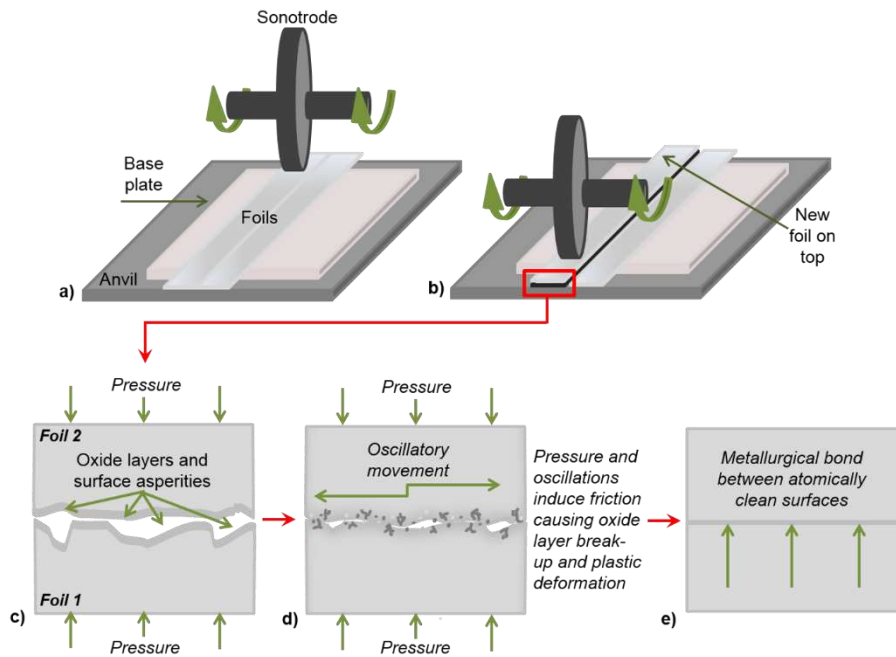


Figure 1. Schematic presentation of the UC process (a) initial welding of foils, (b) welding of foil on top of initial foil and (c) to (e) schematic representation of the bond development at the interface.

Previous research has demonstrated the possibility to embed different fibre types within UC metal matrices² to create smart material structures. The UC process benefits from two key advantages which help to overcome limitations such as high pressures, high temperatures and interfacial reactions which have been observed in well-established metal matrix composite (MMC) manufacturing techniques such as Hot Isostatic Pressing, Diffusion bonding or Thermal Spraying⁴. The first

advantage is that bonding between adjacent metal foils is accomplished at temperatures much lower than the melting temperature of the foil material (typically $\leq 50\%$)⁵. Secondly, the ultrasonic excitation of the metal foil reduces the static yield stress within the material and induces highly localised plastic flow^{3,6}.

Successful fibre integration has been demonstrated for SiC, SMA and optical fibres^{2,7-10}. The bond formation process was demonstrated to be stronger for higher amplitudes and contact pressures^{2,5,8}. Consequently, low pressures and amplitudes entailed unbonded surfaces without encapsulation of the fibres or even separation of the foils. However, higher amplitudes and contact pressures led to distortion and displacement of fibres^{9,11}. For efficient smart material fabrication, higher volume fractions of fibres would be needed for efficient controlling, sensing and actuating. Until now, research on high fibre volume integration has shown that the delivery of sufficient energy to the interfaces was insufficient and led to poor bonding quality^{7,12-13}. To approach high volume fibre integration without high amplitudes yet reducing the required amount of plastic flow and secure and accurate placement of the fibres, a method based on creating trenches in post-UC samples via a laser was pursued. Figure 2 displays the schematic representation of the proposed method. A UC metal substrate was irradiated using a laser to create a channel (Figure 2 a)). The generated molten material was used to be

distributed on the sides of the channel to create raised shoulder features (Figure 2 b)). The shoulders were intended to reduce the required level of plastic flow and enhance encapsulation during consolidation of fibres (Figure 2 c)). The channel itself was intended to securely position the fibres during UC. In Figure 2 c), the intended channel and shoulder geometry is displayed. The geometry was determined as a result of the to-be embedded fibre diameters (100 μm). In Figure 2 d) the final embedded fibre and the UC process is shown.

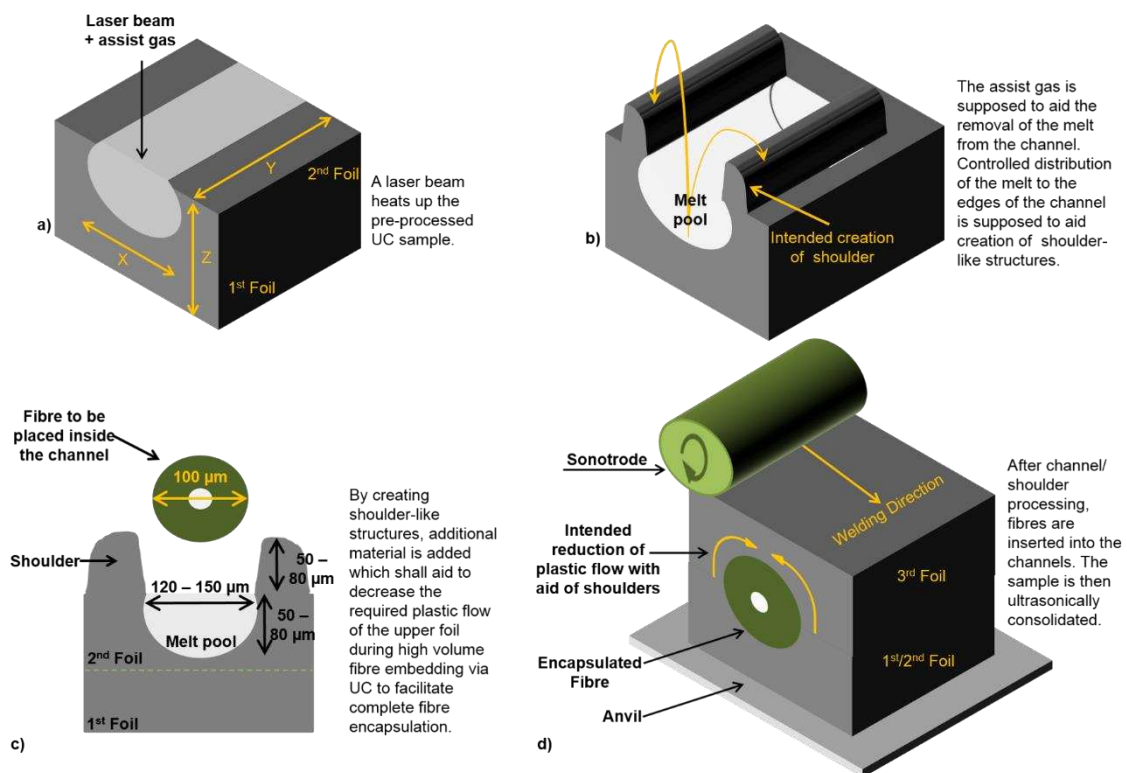


Figure 2. Proposed approach to allow accurate placement and sufficient encapsulation of fibres.

In this study the placement and integrity of SiC fibres placed into the pre-processed laser channels after UC was investigated. Multiple fibres (24) were embedded to investigate the aid of the channels for high volume fibre encapsulation. The authors examined the aid of the channels for accurate fibre placement as well as their integrity after consolidation and the influence of the channel on fibre behaviour.

2. Methodology

2.1 UC sample manufacture

Al 3003-H18 foil (United Aluminium) with a thickness of 100 μm and a width of 25.4 mm was selected as the UC matrix material. Earlier use of the material allowed a comparison of the aid of channels for fibre insertion¹⁴. Prior to laser machining, UC samples were manufactured by using the Alpha 2 UC machine supplied by Solidica INC. The sample production process was similar to that shown in Figure 1. Firstly, an Al 3003-H18 foil was consolidated to an Al 1050 plate (330 x 29 x 1 mm). A second Al 3003-H18 foil was then bonded to the first one to increase the sample thickness (200 μm) prior to laser processing. The parameters used for consolidation of the foils can be seen in Table 1.

Table 1. Parameters for ultrasonically consolidated samples.

Aluminium 3003-H18	Amplitude	Welding Force	Welding Speed	Frequency
-----------------------	------------------	--------------------------	--------------------------	------------------

	20 μm	1400 N	40 mm/s	20 kHz
--	------------------	--------	---------	--------

The UC samples were manufactured at room temperature in an open environment due to an open cabinet.

2.2 Channel processing

Channel processing in post-UC samples was carried out with two different lasers: a SPI 200 W Fiber laser and a Trumpf TruFiber 300 W laser. The main laser specifications are detailed in Table 2.

Table 2. Main laser specifications.

	SPI 200 W Fiber	Trumpf TruFiber 300 W
Wavelength [μm]	1.075	1.085
Beam parameter product [mm.mrad]	0.38	0.4
Focal length [mm]	50	50
Beam propagation factor (M^2)	1.05	1.2
Spot size (calculated) [μm]	13.7	13.1
Irradiance [W/cm^2]	6.78 x 10 ⁷ for 100 W; 1.36 x 10 ⁸ for 200 W	1.48 x 10 ⁸ for 200 W; 2.23 x 10 ⁸ for 300 W

Two different fiber lasers were used as the Trumpf TruFiber 300 W laser exhibited a higher power range compared to the SPI 200 W Fiber laser. Hence, channels manufactured with the Trumpf TruFiber 300 W laser were shown to exhibit a

greater channel depth and higher shoulder features than samples produced by the SPI 200 W fiber laser (see Figure 3). Comparison of the channel depth was considered important for data comparison for effective fibre encapsulation. Additionally, two assist gas types (air and nitrogen) were used for the two lasers in order to compare their influence of the assist gas on UC bond formation in future work. Furthermore, air as an assist gas added an extra ignition source due to the oxygen content which was supposed to aid deep channel production.

Fiber lasers as the laser source were chosen due to the excellent beam quality, the nearly diffraction-limited beam and high brightness, which allowed focusing of the laser to small spot sizes and hence, a high power density input (see Table 2) which was necessary as aluminium exhibits a high reflection coefficient and high thermal conductivity¹⁵⁻¹⁸. The nearly diffraction-limited beam allowed a Gaussian-shaped heat input into the material. It was proposed that higher order modes would modify the heat input into the material, which could possibly make the flow pattern of the melted material more difficult to control¹⁹.

The channel production process has been described elsewhere²⁰. The samples for the SPI 200 W fiber laser were processed using a power of 140 W, a speed of 275 mm/min and a nitrogen gas pressure of 0.6 MPa. The samples for the Trumpf TruFiber 300 W laser were processed using a power of 250 W, a traverse speed of 200 mm/min and an air gas pressure of 0.8 MPa. The parameters were chosen

as they had previously shown the best results for fibre embedding in UC²⁰.

Channels manufactured with the SPI 200 W fiber laser exhibited a depth of 40 to 60 μm and channels manufactured with the Trumpf TruFiber 300 W laser exhibited a depth of 65 to 80 μm . The depth was measured by using a 2 μm inductive gauge (Talysurf CLI 2000 Taylor Hobson Precision) to allow for direct examination. An example of the profile obtained by samples manufactured by the SPI Laser and an example of the profile manufactured by the Trumpf laser can be seen in Figure 3.

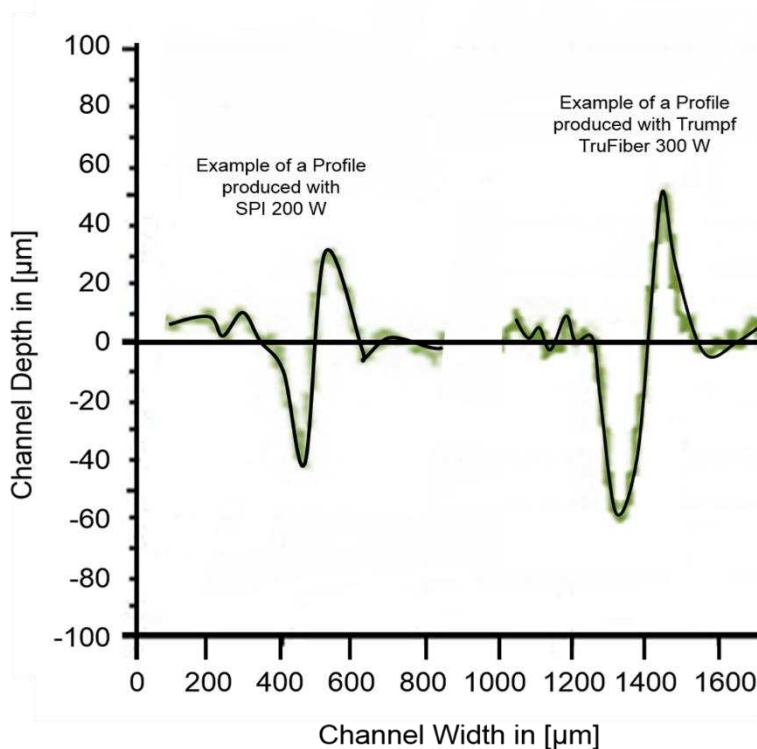


Figure 3. Examples of different channel profiles for SPI 200 W and Trumpf TruFiber 300 W.

As detailed, the shoulder appeared only one-sided. This was due to the flow of the melt and has been previously discussed²⁰. In order to explore the influences of the channel, one-sided shoulder and fibre orientation, which would possibly influence plastic flow behaviour and bond formation during UC⁸, samples containing channels perpendicular and parallel to the welding direction were considered. In Figure 4, both channel types are displayed.

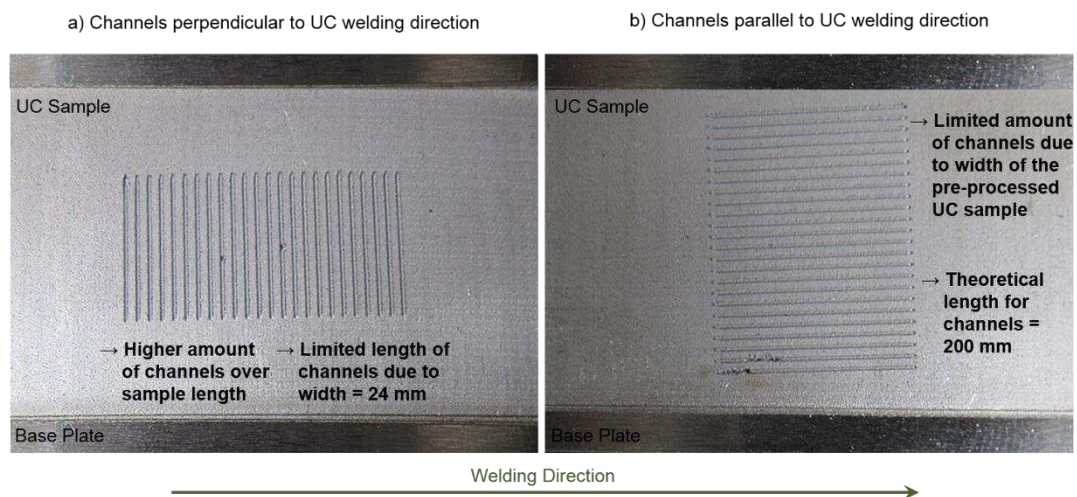


Figure 4. Example of 24 channels manufactured perpendicular to the UC welding direction a) and parallel to the welding direction b).

For channels produced in parallel direction the width of the UC sample (24 mm) limited the amount of channels and shoulders to be produced without interference. Channel production perpendicular to the welding direction limited the length of the channels. Due to these limitations, samples containing 24 channels with a length

of 15 mm were produced. The distance between the channels was set to 750 μm – measured from the starting point of the laser to the edge of the next channel – for samples manufactured with the SPI 200 W laser. Samples manufactured with the Trumpf TruFiber 300 W laser had a distance of 800 μm as the channels exhibited a greater width²⁰. The gap of 750 μm and 800 μm was expected to be necessary to allow a sufficiently big area for bonding of the unprocessed foil material during ultrasonic consolidation.

2.3 Fibre Embedding

To examine the aid of channels and shoulders in terms of fibre positioning and fibre integrity after UC, SiC sigma fibres (QinetiQ, SM-1240) were selected. The fibre consisted of a 10 μm tungsten core and an outer diameter of 100 μm , with a double surface coating of approximately 1 μm titanium boride and 1 μm carbon. The hard nature and high strength of the SiC fibre allowed minimal fibre distortion. A schematic arrangement of the fibre embedding procedure is displayed in Figure 3. The SiC fibres were placed in the channels and held in place by applying adhesive tape (Figure 3(a)). The adhesive tape was applied approximately 1 mm from the end of the channel edges to avoid interference with the fibre embedding analysis. The sample was then placed on the anvil of the UC machine (Figure 5 b)). For samples containing perpendicular channels, the sample was placed with the shoulder in front of the fibre, so that the shoulder would be consolidated first before the sonotrode

can reach the fibre. After that a strip of Al 3003-H18 foil was placed over the fibres (Figure 5 c)).

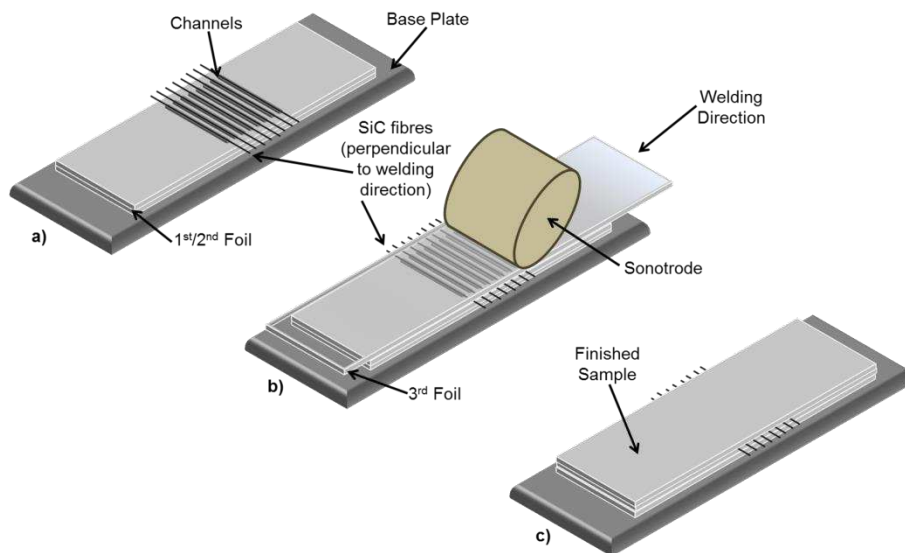


Figure 5. Embedding of fibres within Al 3003-H18 foils: (a) fibre placement, (b) welding of 3rd foil and (c) sample with embedded fibres.

The foil was consolidated by using the same parameters as stated in Table 1. The fibre sample manufacturing was carried out for samples produced by both lasers. Three samples (each containing 24 fibres which corresponds to 10.9 Volume%) for each fibre orientation were produced with the SPI laser and nitrogen (referred to as SPI samples). For the Trumpf laser and air (referred to as Trumpf samples), five samples, also containing 24 fibres (corresponds to 10.2 Volume%), were manufactured for each fibre orientation due an increased depth.

2.4 Microstructural analysis of the samples

To analyse the samples, cross-sectioning of the samples was executed perpendicular to the channel direction with a diamond blade (Series 15HC Diamond) (Buehler Isomet Low Speed Saw) to avoid any possible cutting induced fibre damage. The samples were mounted into Buehler Konductomet II. The surface was ground to a surface finish of 1 μm Ra and then polished with colloidal silica to a surface finish of 0.1 μm Ra. Optical microscopy was conducted using an Olympus BX 60M microscope equipped with a MicroPublisher 3.3 RTV digital camera. A magnification of x 100 was used.

To determine the aid of the channels for accurate positioning and to analyse the fibre appearance post UC in greater detail, a Carl Zeiss 1530VP (Leo, Cambridge) scanning electron microscope (SEM) was used. To analyse the position of the fibres post UC, the distance between the centres of two fibre cores was measured. The fibre core of a SiC fibre appeared as a bright point during SEM and was therefore readily distinguishable. Measurements were carried out by using point-to-point analysis with the LEO 32 user interface which allowed accurate measurement of the distance between the fibre cores. Distance measurement was carried out for three samples (72 fibres) in perpendicular and three samples (72 fibres) in parallel direction for each gas type. As the channel distances were set to 750 μm and 800 μm , the distance between the fibres cores was intended to be in the same range as

the fibres had a diameter of 100 μm . The average values for the three samples in parallel and the three samples in perpendicular direction were then compared to each other. To analyse the fibre appearance post UC, fibres were inspected by using different magnifications. Energy dispersive X-ray spectroscopy (EDX) maps were taken to specify the main elements for alloy and fibre. The EDX was integrated in the SEM and an Oxford Instruments X-Max 80 mm^2 detector was used. The beam current was set to 20 keV.

3. Results and Discussion

3.1 Accurate positioning of fibres

Analysis of accurate positioning of fibres after UC was carried out in order to determine the assistance of the channels (and shoulders) from preventing rolling or movement of fibres during UC. When embedding high quantities of fibres, movement or rolling is not desirable as fibres may come into contact with each other or prohibit sufficient bonding area between the foils.

The average distances of the three parallel and the three perpendicular samples for samples manufactured with the SPI laser are shown in Figure 6. The average distance for all samples containing fibres placed in parallel direction was 722 μm . The average distance for all perpendicular samples was similar (724 μm), yet

lower than the original distance set between the fibres (750 μm). It can be seen from the diagram that the average values alternated around the mean average. However, the average of the perpendicularly embedded fibres ranged in a wider distance (560 to 820 μm) than parallel embedded fibres (655 to 800 μm). Hence, fibres embedded in parallel direction were less likely to move than perpendicularly embedded fibres.

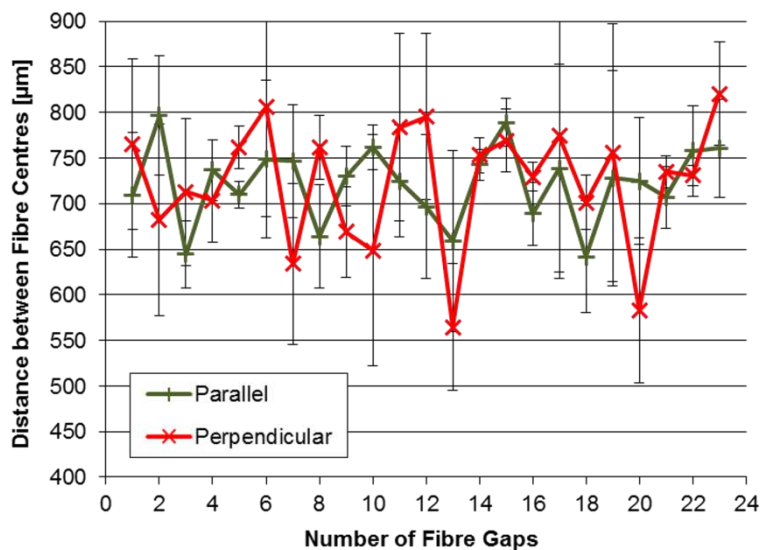


Figure 6. Average distance between fibre cores for both orientations (SPI 200 W; nitrogen).

The average distances of the five parallel and the five perpendicular samples for samples manufactured with the Trumpf laser are shown in Figure 7. The mean average for all the fibres embedded in parallel direction was 818 μm ; the mean average for fibres embedded in perpendicular direction was 788 μm . The average

values of both directions were fluctuating around the set distance of 800 μm .

Compared to the SPI samples in Figure 6, the overall distance between the fibre centre averages was more consistent.

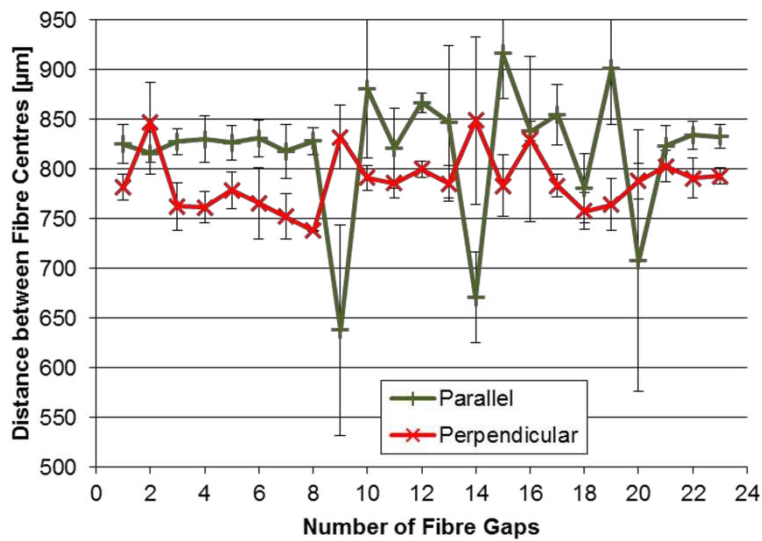


Figure 7. Average distance between fibre cores for both orientations (Trumpf TruFiber; air).

However, opposed to the results for the SPI laser samples, the Trumpf samples showed that especially parallel fibres showed a wider range (640 μm to 920 μm) whereas perpendicular embedded fibres ranged from 740 μm to 850 μm . The reason for the greater range for parallel fibres was possibly that fibres moved out of the channel due to their propensity to roll and the dynamic forces applied from the sonotrode which will be discussed later on. Furthermore, as can be seen for example for fibre 9 and 10 in Figure 7: as one fibre was displaced from the channel,

the distance to the following fibre got shorter and increased the distance to the other adjacent fibre.

Little current knowledge exists about the secure and accurate positioning of fibres. To date most studies have focused on the plastic behaviour of the material encapsulating the fibres while the fibres were being held in place by clamping mechanisms. Kong²¹ found that fibres in close proximity can disturb each other while also impeding the bond formation process during UC⁹. In Figure 8 a) an example of a high quantity of fibres in an Al 3003-H18 matrix without channels is shown. The fibres were not evenly distributed and in some cases in direct contact with each other. The reason for this was that fibres are moving due to the applied oscillations and pressure if not secured. Contact of the fibres could present a problem when using delicate fibres such as optical fibres which can easily lose their ability to guide light when breaking. Furthermore, uneven spacing could lead to difficulties when embedding multiple fibre types. In Figure 8 b), SiC fibres embedded in channels after consolidation in this study can be seen. Compared to the fibres in Figure 8 a), the fibres were, due to the channel, restricted in moving and stayed in the channels after consolidation. Furthermore, the fibres were evenly distributed over the matrix interface.

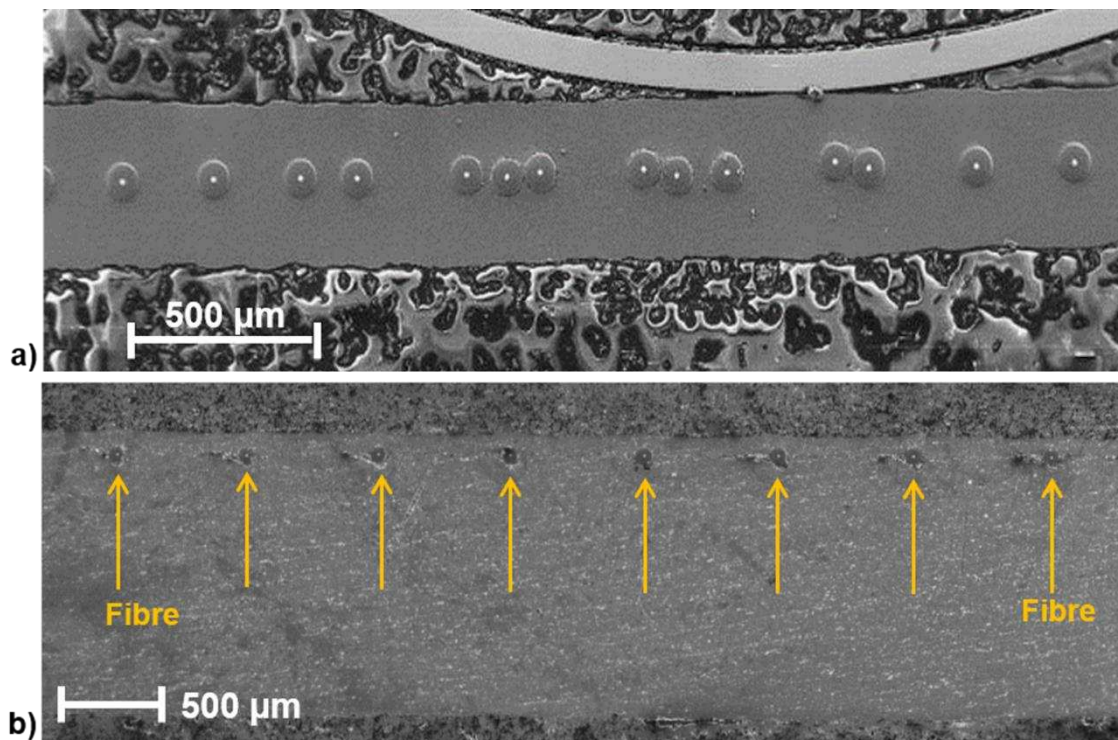


Figure 8. High quantity of SiC fibres within an Al 3003-H18 matrix [21] without channels after UC a) and with channels b).

To clarify the aid of the channels for accurate positioning, all fibres were analysed via SEM inspection. The results can be seen in Table 3. The results revealed that fibres in SPI laser samples were less likely to stay in the channels after UC. Only 72% for parallel embedded fibres and 63% for perpendicular embedded fibres were found to be in the channel. The results for Trumpf samples indicated that for both directions over 90% of the fibres remained in the channels after UC, with

perpendicular embedded fibres reaching a value of 98%. Hence, only two of the 120 fibres moved out of their channel.

Table 3. Analysis of fibre positioning for nitrogen and air samples for both directions.

Fiber laser type	Embedding Direction	Total number of Embedded Fibres	No of Fibres in Channel	Percentage of Fibres in Channel
SPI	Parallel	72	52	72.2%
	Perpendicular	72	46	63.9%
Trumpf	Parallel	120	109	90.8%
	Perpendicular	120	118	98.3%

In Figure 9, an example for fibre movement is presented.

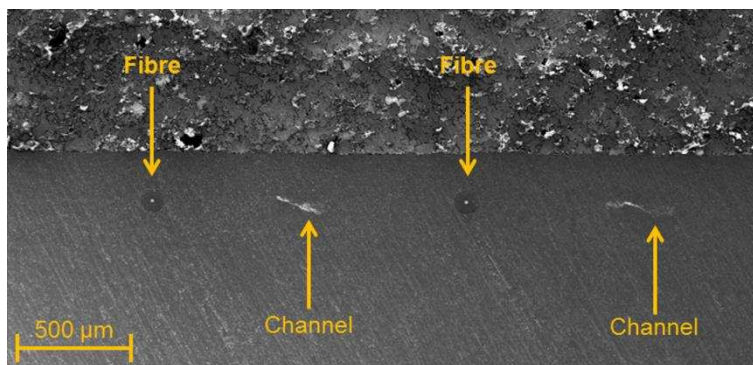


Figure 9. Fibres not embedded in channels after UC

This behaviour was observed for nearly 30% of the fibres embedded in parallel direction and for nearly 40% of perpendicular embedded fibres for samples

processed with the SPI laser. Hence, accurate positioning was difficult to control. The reason for the movement of the fibres for SPI samples during UC was the lack of sufficient channel depth. Compared to the channels produced with the Trumpf laser which exhibited a channel depth of 65 to 80 μm , the channel depth for nitrogen samples was only in the range of 40 to 60 μm . Furthermore, the embedding direction may have influenced the movement of fibres which could explain a difference in movement for both directions for SPI samples. Parallel embedded fibres received the normal force and oscillations from the sonotrode over their whole length during UC, whereas perpendicularly embedded fibres received the normal force and oscillations over their diameter as schematically displayed in Figure 10.

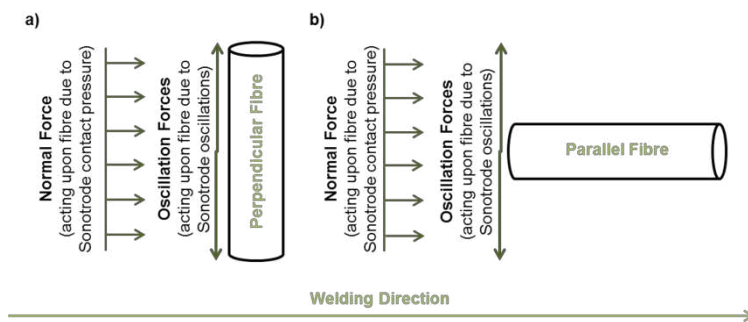


Figure 10. Dynamic forces acting on (a) perpendicular fibre and (b) on parallel fibre with regards to welding direction.

It was suggested that the perpendicular fibres in combination with a smaller depth were, due to the normal applied force, pushed along the welding direction.

Furthermore, the rolling direction of the fibres was in favour to move along the welding direction.

On the contrary, Trumpf samples showed that perpendicular embedded fibres gave better results. It was anticipated that, due to the deeper channels, the oscillation force was the main influence on fibre movement which made the fibres oscillate around their genuine rolling direction. Hence, depending on a channel existence and the depth, either normal or oscillation force may act on the fibres.

3.2 Aid of channels and shoulders for integrity of fibres after UC

Channel and shoulder manufacturing into the metal matrices was intended to meet two conditions: Firstly, the accurate placement of fibres and secondly, preventing damage keeping of the fibres during UC. To analyse the second condition, all fibres were closely inspected to analyse their integrity after UC.

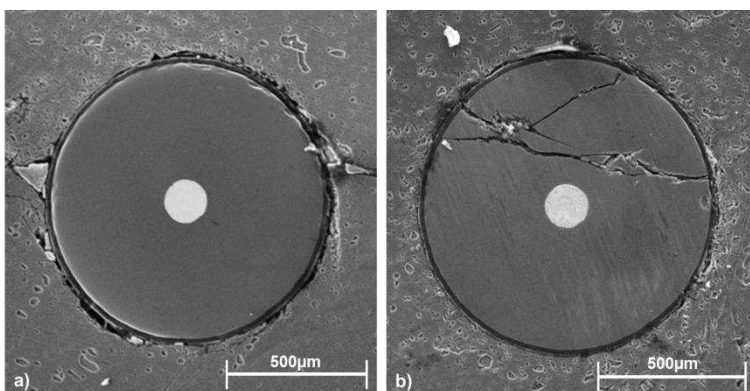


Figure 11. a) Intact embedded fibre and b) embedded cracked fibre after UC

In Figure 11 a) and b) an intact fibre and a fibre exhibiting cracks are displayed. The degree of cracking varied from sample to sample, however every sample exhibited at least one cracked fibre. The severity of the cracking varied. Analysis of the cracked fibres and their relation to movement of the fibres was carried out by calculating the percentage of cracked fibres. The results are displayed in Table 4.

Table 4. Analysis of fibre cracking for all fibres.

Fiber laser type	Embedding Direction	Total of Embedded Fibres	No of Fibres in Channel	No of Cracked Fibres	Percentage of Cracked Fibres
SPI	Parallel	72	52	8	11.1%
	Perpendicular	72	46	6	8.3%
Trumpf	Parallel	120	109	5	4.2%
	Perpendicular	120	118	4	3.3%

As already seen from the results for fibre movement, Trumpf samples exhibited superior results than SPI samples. The percentage of cracked fibres in parallel direction was 4.2% and 3.3% for perpendicular places fibres. For parallel embedded SPI samples the percentage of cracked fibres was over 10% and a little less in perpendicular direction. It was noticed that for both laser types, the percentage of cracked fibres was higher for parallel embedded fibres. A possible reason for cracking in parallel direction may have been the dynamic forces such as normal and

oscillating forces acting on the fibre (see Figure 10). As discussed before, a parallel embedded fibre would get the forces over the whole fibre length. A perpendicular embedded fibre receives the forces also over the whole length; however, the interaction time is less than for a parallel fibre which could enforce the development of cracks. Another reason for fibre cracking, especially for SPI samples, may have been the correlation between movement of fibres and cracking of fibres. Moving out of the channel increased the force exerted on the fibre by the sonotrode making the fibres more susceptible to cracking due to the applied forces during UC.

In Figure 12, a representative EDX map of the main alloying elements in the matrix material and the fibre elements are given.

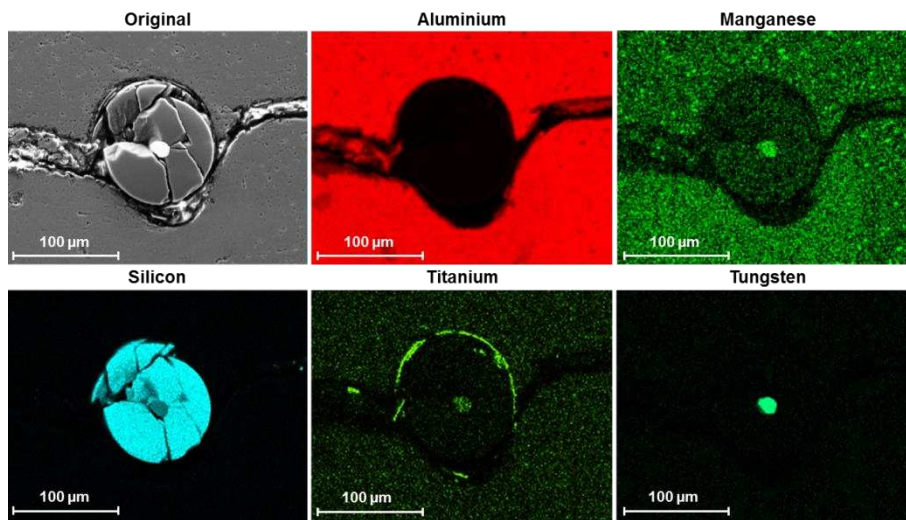


Figure 12. EDX mapping of elements around broken fibre

EDX was carried out to understand the distribution of the cracked fibre in relation to the welding direction and welding forces. The results showed that the damaged fibres which stayed in the channel were distributed within the channel rather than along the weld line as can be seen for silicon and titanium. A possible explanation for fibre cracking in the channel may have been a combination of normal force with simultaneous hardening of the channel bottom due to laser processing. Hence, the fibre was exposed to pressure from the top and a hard surface from the bottom which led to fibre cracking via fibre compression. Research on fibre damage during UC has never been reported before for SiC fibres. However, reference samples without channels but containing the same amount of fibre volume also showed fibre damage. This was suggested to be another indication for damage occurring due to the dynamic forces imposed during UC. Further research on fibre breakage is currently investigated to clarify which influence is causing the damage.

4 Conclusions

This study demonstrated a novel and unique approach to advance UC as a manufacturing process for high volume fibre integration. Compelling evidence for the aid of the laser manufactured channels to accurately position high volume fractions of fibres was observed for samples which exhibited an increased channel depth (Trumpf) as opposed to less deep channels (SPI). Over 90% of the parallel

embedded fibres (9.2 Volume%) manufactured with the Trumpf laser were observed to remain in the channel after UC. For perpendicular placed fibres 98% (10 Volume%) of the fibres remained in the channel. For perpendicular placed fibres in SPI manufactured samples only 63.9 % and 73 % for parallel placed fibres stayed in the channel which was concluded to be due to the smaller channel depths. Hence, laser processed channels can enhance the accurate distribution of fibres within a metal matrix composite which aids the further development of the UC process as a metal matrix manufacturing process.

The study of the preservation of fibre integrity after UC showed that every sample exhibited fibre damage. Up to 11% of the fibres embedded in SPI samples were damaged and up to 4% of the fibres embedded in Trumpf samples were damaged which may be attributed to the different channel depths. Furthermore, fibres embedded parallel to the welding direction were more easily damaged than fibres in perpendicular direction. It was suggested that dynamic forces over the whole fibre length (parallel) caused more fibre damage due to the longer interaction time during UC. Additionally, it was suggested that the microstructure of the channel surface may have had an influence on fibre breakage. Further investigations to identify the catalyst for fibre damage will be carried out. The influence of the embedding direction on fibre damage has been investigated for the first time and contributes to

the further understanding of the dynamic forces induced on delicate materials with regards to future embedding research and application.

Acknowledgments

The authors gratefully acknowledge the financial support of the EPSRC/IMCRC through grant number EPSRC IMCRC 275.

References

1. White DR. Ultrasonic Consolidation of Aluminium Tooling. *Adv Mater Process* 2003; 161(1):64-65.
2. Kong CY, Soar RC. Fabrication of metal–matrix composites and adaptive composites using ultrasonic consolidation process. *Mater Sci Eng A Struct Mater* 2005; 412:12–18.
3. Yang Y, Janaki Ram GD, Stucker BE. Bond formation and fiber embedment during ultrasonic consolidation. *J Mater Process Technol* 2009; 209:4915–4924.
4. Clyne TW, Withers PJ. *An introduction to metal matrix composites*. Cambridge: Cambridge University Press, 1993.
5. Kong CY. Ultrasonic consolidation for embedding SMA fibres within aluminium matrices. *Compos Struct* 2004; 66(1-4):421-427.
6. Langenecker B. Effects of ultrasound on deformation characteristics of metals. *IEEE Transactions on Sonics and Ultrasonics* 1966; 13(1):1-8.
7. Li D, Soar, RC. Characterization of Process for Embedding SiC Fibers in Al 6061 0 Matrix Through Ultrasonic Consolidation. *J Eng Mater Technol* 2009; 131:021016-1-021016-6.

8. Yang Y, Janaki Ram GD, Stucker BE. An Experimental Determination of Optimum Processing Parameters for Al/SiC Metal Matrix Composites Made Using Ultrasonic Consolidation. *J Eng Mater Technol* 2007; 129(4):538-549.
9. Friel RJ, Harris RA. A nanometre-scale fibre-to-matrix interface characterization of an ultrasonically consolidated metal matrix composite. *Proc Inst Mech Eng L J Mater Des Appl* 2009; 224:31-40.
10. Kong CY, Soar RC. Method for embedding optical fibers in an aluminium matrix by ultrasonic consolidation. *Appl Opt* 2005; 44(30):6325-6333.
11. Hahnen R, Dapino MJ. Active Metal-matrix Composites with Embedded Smart Materials by Ultrasonic Additive Manufacturing. In: *Proc. of SPIE Vol. 7645*. San Diego, March, 2010. p.76450O-1-76450O-12.
12. Kong CY, Soar RC, Dickens PM. Optimum process parameters for ultrasonic consolidation of 3003 aluminium. *J Mater Process Technol* 2004; 146:181–187.
13. Friel RJ, Johnson KE, Dickens PM, Harris RA. The effect of interface topography for Ultrasonic Consolidation of aluminium. *Mater Sci Eng A Struct Mater* 2010; 527:4474–4483.
14. Yang Y, Stucker BE, Janaki Ram GD. Mechanical Properties and Microstructures of SiC Fiber-reinforced Metal Matrix Composites Made Using Ultrasonic Consolidation. *Compos Struct* 2010; 44(26):3179-3194.
15. Tünnermann A, Schreiber T, Röser F, Liem A, Höfer S, Zellmer H, Nolte S, Limpert J. The renaissance and bright future of fiber lasers. *J Phys B At Mol Opt Phys* 2005; 38:S681-S693.
16. Limpert I, Liem A, Zellmer H, Tuennermann A. 500 W continuous-wave fibre laser with excellent beam quality. *Electron Lett* 2003; 39(8):645-647.

17. Beyer E, Mahrle A, Lütke M, Standfuss J, Brückner F. Innovation in high power fiber laser applications. In. Fiber Lasers IX: Technology, Systems, and Applications, edited by Eric C. Honea, Proc. of SPIE Vol. 8237,823717-1-823717-11.
18. Riviero A, Quintero F, Lusquinos F, Comesana R, Pou J. Parametric investigation of CO2 laser cutting of 2024-T3 alloy. J Mat Process Technol 2010; 210:1138-1152.
19. Han L, Liou FW. Numerical investigation of the influence of laser beam mode on melt pool. Int J Heat Mass Tran 2004; 4747:4385–4402.
20. Masurtschak S, Friel RJ, Gillner A, Ryll J, Harris RA. Fiber Laser Induced Surface Modification/Manipulation of an Ultrasonically Consolidated Metal Matrix. J Mat Process Technol 2012; 213:1792-1800.
21. Kong CY. Investigation of ultrasonic consolidation for embedding active/passive fibres in aluminium matrices. PhDThesis, Loughborough University, UK, 2005.